Neutron diffraction study of $TbMnO_3$: Magnetic structure revisited

R. Kajimoto
Neutron Science Laboratory, Institute of Materials Structure Science, High Energy Accelerator Research Organization (KEK), 1-1 Oho, Tsukuba, Ibaraki 305-0801, Japan

H. Yoshizawa
Neutron Science Laboratory, Institute for Solid State Physics, University of Tokyo, Tokai, Ibaraki 319-1106, Japan

H. Shintani, T. Kimura,* and Y. Tokura
Department of Applied Physics, University of Tokyo, Bunkyo-ku, Tokyo 113-8656, Japan

(Dated: February 6, 2008)

Magnetic ordering in $TbMnO_3$ was revisited by a neutron diffraction study. In addition to the previously reported A-type and G-type modulated structures with a propagation vector $(0, q_{\rm Mn}, 0)$,[1,2] we found C-type and F-type orderings of the Mn moments. All the components appear below $T_N^{\rm Mn} = 46$ K, and the G, C, and F-type components are enhanced below $T_{\rm lock} = 28$ K, where $q_{\rm Mn}$ ordering locks at its low temperature value. The locking of the propagation vector also yields the squaring up of the spin arrangement. The magnetic moments of Tb ions show a quasi long-range ordering below $T_N^{\rm Tb} = 7$ K. It drastically promotes the development of the G, C, and F-type components while suppressing the A-type components.

PACS numbers: 75.47.Lx, 75.25.+z

Perovskite manganese oxides $R\mathrm{MnO_3}$ (R = trivalent rare earth ion) are famous as the parent materials of the colossal magnetoresistive manganites. The Mn ions in $R\mathrm{MnO_3}$ become trivalent having the $t_{2g}^3 e_g^1$ configuration. This electronic configuration induces a degree of freedom of the e_g orbital, which produces many novel properties. In the most well studied material, $\mathrm{LaMnO_3}$, the e_g orbitals form staggered ordering of $d_{3x^2-r^2}$ and $d_{3y^2-r^2}$ orbitals, which induces the layered-type (so-called A-type) antiferromagnetic ordering of Mn spins. In contrast, when the ionic radius of R is substantially small, $R\mathrm{MnO_3}$ shows a modulated spin ordering with a propagation vector $(0, q_{\rm Mn}, 0)$ (in the orthorhombic $Pbnm$ cell).[1,2,3,4,5] The emergence of the incommensurate spin structure is explained as a competition between the nearest-neighbor (NN) spin interactions and the next-nearest-neighbor (NNN) interactions caused by the combination of the $\mathrm{GdFeO_3}$-type distortion and the $d_{3x^2-r^2}/d_{3y^2-r^2}$ orbital ordering (We will refer to this model as the NN-NNN model.).[6]

$TbMnO_3$ is one of the latter series of $R\mathrm{MnO_3}$. It shows an incommensurate sinusoidal spin ordering with $q_{\rm Mn} \sim 0.295$ below $T_N \sim 41$ K with spins oriented along the [010] direction. $q_{\rm Mn}$ decreases as temperature is lowered, then locked at $q_{\rm Mn} = 0.28$ below $T_{\rm lock} \sim 30$ K.[1] Very recently, it was found that the spontaneous electric polarization P parallel to the c axis appears below $T_{\rm lock}$.[7] Moreover, the magnitude or the direction of P can be drastically changed by applying a magnetic field.[7] The magnetic control of the ferroelectric polarization will provide an attractive possibility of new magnetoelectric devices.

These recent discoveries in the $R\mathrm{MnO_3}$ series motivated us to reinvestigate the magnetic properties of these materials in detail. Here, we report the result of a neutron diffraction study on the elastic properties of the magnetic ordering in $TbMnO_3$. The study of the inelastic properties by neutron scattering is underway, and will be published elsewhere.[8]

A single crystal of $TbMnO_3$ was grown by the floating zone method. A detailed procedure of the sample preparation was described elsewhere.[7] The neutron diffraction experiments were performed using the triple axis spectrometer GPTAS installed at the JRR-3M research reactor in JAERI, Tokai, Japan. A neutron wave length of $k_i = 2.57$ Å^{-1} was selected by the 002 reflection of a pyrolytic graphite (PG) monochromator. The horizontal collimation of 40′-40′-40′-blank (from monochromator to sample) was used for most of the measurements, while the 20′-20′-20′-blank collimation was utilized for the investigation of temperature dependence of the wave vector of the magnetic ordering. Two PG filters were placed before the monochromator and after the sample to suppress contaminations of higher-order harmonics. The crystal structure has the $Pbnm$ symmetry, and the measurements were performed in the $(0kl)$ scattering plane ($a^* = 1.08$ Å^{-1} and $c^* = 0.853$ Å^{-1}). The sample was mounted in an aluminum can filled with helium gas, and was attached to the closed-cycle helium gas refrigerator. All the temperature dependence data were collected upon heating to avoid uncertainty due to the hysteresis.

First, we surveyed magnetic reflections in the $(0kl)$ scattering plane with the relaxed collimation (40′-40′-40′-blank). Figure 1 shows neutron scattering profiles along the $(0, k, 0)$ and $(0, k, 1)$ lines at 4 K, 10 K, and 55 K. At 4 K, surprisingly many superlattice reflections due to the magnetic moments of both Mn and Tb ions are observed at every position with $k \approx n/7$ (n = integers). At 10 K,

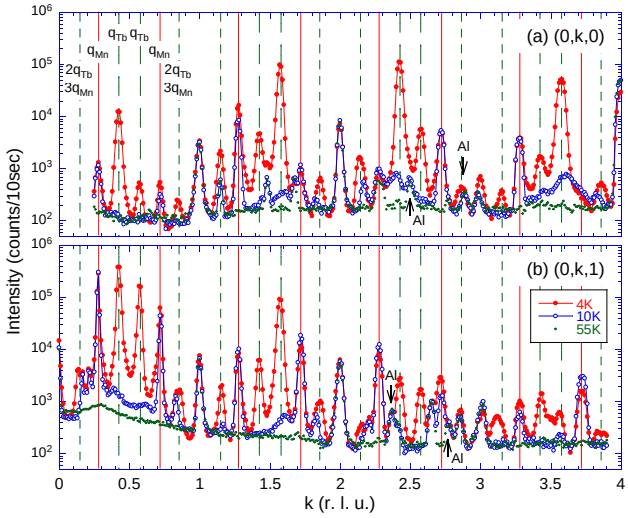

FIG. 1: (Color online) Neutron diffraction profiles along (a) the $(0, k, 0)$ line and (b) the $(0, k, 1)$ line at 4, 10, and 55 K. Vertical lines indicate the positions of the Mn ($k \approx$ integer $\pm$ 2/7 and 6/7) and Tb ($k \approx$ integer $\pm$ 3/7 and 6/7) superlattice peaks. "Al" denotes diffractions from the aluminum sample cell.

on the other hand, only the Mn peaks are observed with broad peaks coming from the short-range order of the Tb moments.

The magnetic reflections due to the Mn ordering were observed at $(h, k \pm q_{\rm Mn}, l)$ with $q_{\rm Mn} = 0.28$, where solid vertical lines are drawn in Fig. 1. The observed Mn peaks can be classified into five groups depending on the values of h, k, and l as A-type ($h + k$ = even and l = odd), G-type ($h + k$ = odd and l = odd), C-type ($h + k$ = odd and l = even), and F-type ($h + k$ = even and l = even). Quezel *et al.* observed strong A-type reflections and weak G-type peaks, but they did not observe any C-type and F-type reflections.[1] They concluded that the A-type peaks come from a sinusoidally modulated spin ordering with spins parallel to the b axis. In contrast to Quezel's result, we observed clear peaks of both C-type and F-type in addition to the A-type and G-type peaks. Since the small number of the observed magnetic peaks prevents us to unambiguously determine the real space spin configuration, we just performed a preliminary analysis of the magnetic structure: We calculated the intensities for the sinusoidal and the helical spin configurations assuming the spins lie on the ab, bc, or ca planes, and compared them with the observed intensities at 10 K. The intensities of the A-type peaks are best described by the sinusoidal model with spins parallel to the b axis as reported by Quezel *et al.* Analysis of the G-type peaks gave the similar result. For the C-type and F-type peaks, however, we failed to satisfactorily reproduce the observed intensities, though the existence of the peaks on the $(0, k, 0)$ line indicates the spin arrangements have substantial x or z components.

Figures 2(a)-(d) show temperature dependences of the

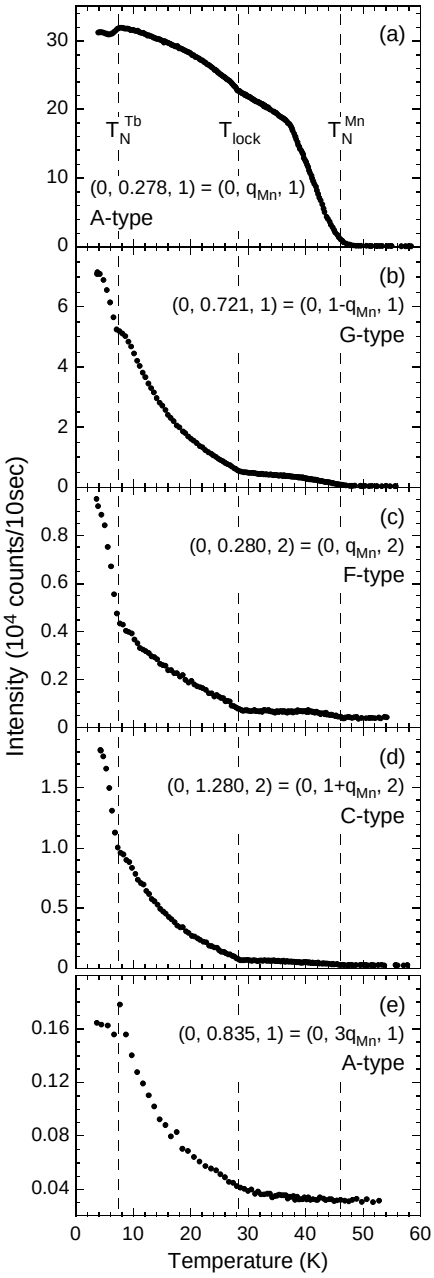

FIG. 2: (a)-(d) Temperature dependences of the intensities of the Mn superlattice peaks of (a) A-type, (b) G-type, (c) F-type, and (d) C-type. (e) Temperature dependence of the intensity of the Mn third harmonics at $(0, 0.835, 1) = (0, 3q_{\rm Mn}, 1)$.

scattering intensities of the Mn magnetic peaks. Each panel corresponds to the superlattice peak of (a) A-type: $(0, 0.278, 1) = (0, q_{\rm Mn}, 1)$, (b) G-type: $(0, 0.721, 1) = (0, 1 - q_{\rm Mn}, 1)$, (c) F-type: $(0, 0.280, 2) = (0, q_{\rm Mn}, 2)$, and (d) C-type: $(0, 1.280, 2) = (0, 1 + q_{\rm Mn}, 2)$. All the intensities start to increase at $T_N^{\rm Mn} = 46$ K, which is slightly higher than the reported transition temperatures.[1,2,6] There are two distinct anomalies in the temperature profiles below $T_N^{\rm Mn}$: with decreasing temperature, the slopes

show upturns at $T_{\rm lock} = 28$ K, and then a drastic drop of the A-type peak (a) or increases of the others (b)-(d) below $T_N^{\rm Tb} = 7$ K. The former temperature coincides with the temperature where the wave vector of the Mn ordering locks at its low temperature value as described later. The latter anomaly is concomitant with the ordering of the Tb moments (see below). All the weak (G, C, and F) components show a similar temperature dependence, and they gradually develop below $T_N^{\rm Mn}$. Their temperature dependence is quite different from the sharp increase of the A-type component, suggesting that the weak components arise from some secondary effect. One of probable causes is the development of the ordering of the Tb moments, which is manifested by the steep increase of these components in compensation for the A-type component on the (quasi) long-range ordering of the Tb moments (Fig. 2).

In addition to the fundamental ($1q_{\rm Mn}$) peaks described above, we also observed the third harmonics ($3q_{\rm Mn}$) of each type of the Mn ordering at $(h, k \pm 3q_{\rm Mn}, l)$ (dashed lines in Fig. 1). Though we could not detect the third harmonics for the F-type ordering, it may be because of the weakness of the fundamental ($1q_{\rm Mn}$) F-type peaks. The existence of the higher harmonics of the Mn ordering means that the spin ordering is not an ideal sinusoidal wave. The ratio of the intensity of the $3q_{\rm Mn}$ peak to that of the $1q_{\rm Mn}$ peak is $\sim 10^{-2}$. This value is much smaller than that for an ideal square wave (1/9), indicating the deviation of the spin arrangement from the sinusoidal wave is quite small. Nevertheless, the existence of the higher harmonics is interesting in that the NN-NNN model predicts the square ordering of the Ising-like spins.[6] In Fig. 2(e) is shown the temperature dependence of the intensity of the $3q_{\rm Mn}$ peak of the A-type ordering. It gradually develops below $T_{\rm lock}$, indicating that the sinusoidal ordering pattern of the Mn moments becomes distorted at $T < T_{\rm lock}$.

The superlattice peaks due to the ordering of the Tb moments were observed at $(h, k \pm q_{\rm Tb}, l)$ with $h, k, l =$ integer and $q_{\rm Tb} = 0.42$ (dotted-and-dashed lines in Fig. 1). The Tb peaks are observed in all zones similar to the Mn ordering. Though the previous study on a single crystal reported the Tb peaks are broad and less intense compared to the Mn peaks,[1] we observed quite sharp and much intense peaks at the lowest temperature. Figure 3(a) shows the temperature dependence of the Tb peak intensity at $(0, 0.424, 1) = (0, q_{\rm Tb}, 1)$. It shows a steep increase below $T_N^{\rm Tb} = 7$ K. In addition, superlattice peaks are observed at $k \pm 0.15$ in all zones (dashed lines in Fig. 1). The intensity of these peaks shows the same temperature dependence as the Tb peaks [Fig. 3(b)], indicating that these peaks are related to the Tb ordering. Since the positions of the superlattices correspond to $2q_{\rm Tb}$, these peaks may be attributed to the second harmonics of the Tb ordering. The existence of the even harmonics means a space symmetry breaking.[9] On the other hand, a magnetic ordering can induce the second harmonics of lattice origin.[10] The exact origin of the peaks at $2q_{\rm Tb}$ remains an open question.

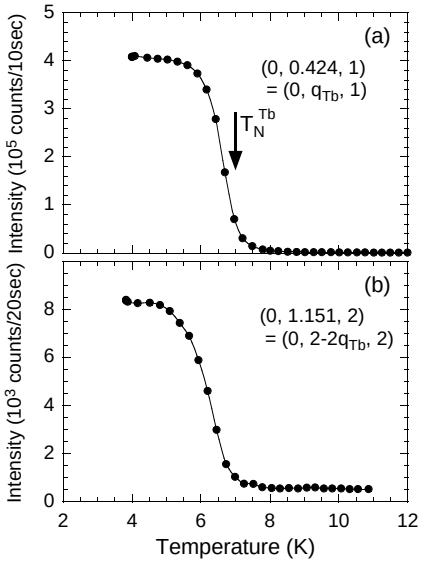

FIG. 3: Temperature dependences of the peak intensities due to the Tb ordering at (a) $(0, 0.424, 1) = (0, q_{\rm Tb}, 1)$ and (b) $(0, 1.151, 2) = (0, 2 - 2q_{\rm Tb}, 2)$.

Next, we measured temperature dependence of a profile of an A-type Mn peak to derive the change of the wave vector of the Mn spin ordering as a function of temperature. The NN-NNN model predicts that the wave number shows a step-wise temperature variation as locking at certain rational values.[6] In the previous diffraction measurements, however, only a smooth temperature dependence below $T_{\rm lock}$ was observed,[1,6] suggesting that the effect of the locking is, if it exists, relatively weak. In the present study, we collected the temperature dependence data at substantially fine intervals of temperature ($\Delta T \sim 0.5$ K) with the tight collimation (20′-20′-20′-blank) to detect small anomalies in the wave vector of the Mn ordering. With this condition, the widths of the Mn peaks are still resolution limited for both the [010] and the [001] directions, while the Tb peaks have finite intrinsic widths. The correlation lengths of the Tb ordering, which is derived from the peak width of $(0, q_{\rm Tb}, 1)$ peak at 5 K by assuming a Gaussian line shape and deconvoluting the resolution, is $\sim$140 Å both along the [010] and [001] directions.

We show in the inset of Fig. 4(a) the temperature variation of the profile of the Mn peak at $(0, q_{\rm Mn}, 1) \approx (0, 0.28, 1)$. One can see clearly the peak position shifts toward higher Q as the temperature increases. By fitting these data to Gaussians (solid lines in the figure), we extract the temperature dependence of the peak height, the peak position (the wave number $q_{\rm Mn}$), and the peak width (full width at half-maximum, FWHM), which are summarized in Fig. 4. With increasing temperature, the peak intensity shows an increase at $T < T_N^{\rm Tb} = 7$ K, then decreases [Fig. 4(a)]. The slope of the temperature profile exhibits an inflection

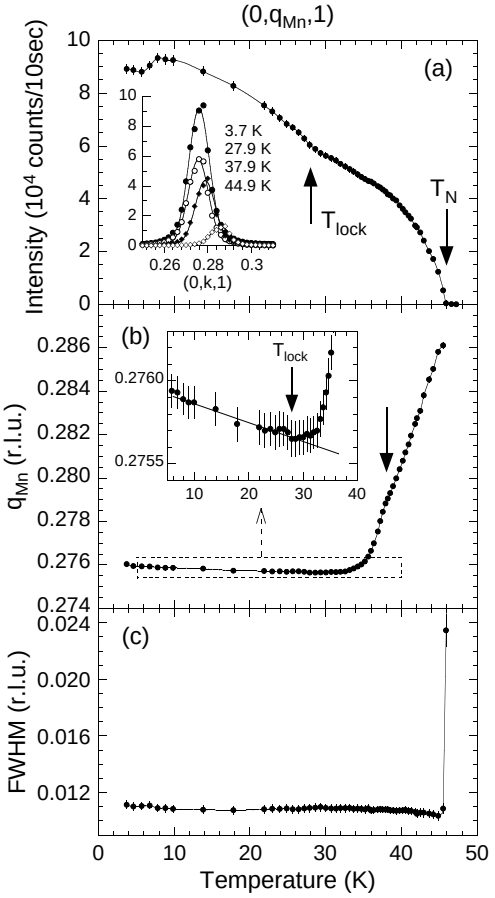

FIG. 4: Temperature dependences of (a) the peak intensity, (b) the wave number, and (c) the peak width of the Mn $(0, q_{\rm Mn}, 1)$ peak. Inset of panel (a): Temperature dependence of the Mn peak profile at $(0, q_{\rm Mn}, 1)$ along the [010] direction.

at $T_{\rm lock} = 28$ K. Finally, the intensity vanishes at $T_N^{\rm Mn} = 46$ K. For the wave number $q_{\rm Mn}$, it is nearly constant at 0.276 r.l.u. (reciprocal lattice unit) $\approx 5/18$ (or $11/40$) r.l.u. at low temperature with a slow decrease as a function of temperature [Fig. 4(b)]. It shows a steep rise above $\sim$34 K, but the upturn of the wave number starts at $T_{\rm lock}$ [inset of Fig. 4(b)]. It changes the slope of its temperature dependence at 38 K, then it increases monotonically without any locking behavior. For the peak width, it is resolution limited below $T_N^{\rm Mn}$, and diverges above $T_N^{\rm Mn}$ [Fig. 4(c)]. We also measured temperature dependence of the profile along the [001] direction, but did not find any anomalies.

According to the NN-NNN model, the wave number of the Mn ordering $q_{\rm Mn}$ decreases in a step-wise manner as lowering the temperature, and reaches zero in the ground state. However, the step-wise behavior is indistinct and $q_{\rm Mn}$ locks at the finite value below $T_{\rm lock}$ in the real material, although the observed temperature dependence of $q_{\rm Mn}$ semiquantitatively agrees with the model. This means some higher order effects than the NN and NNN spin interactions that stabilize the modulated structure must be considered. The coupling between the Mn moments and the Tb moments may play a role, but it fails to explain the fact that the similar incommensurate spin ordering and the locking behavior at the low temperature were also observed in orthorhombic $YMnO_3$, where the rare earth ion has no magnetic moment.[5] Further studies are needed to solve this problem, and the study of the dynamics will be helpful.

To sum up the present study, we have investigated the ordering of the Mn and Tb moments in a single crystal of $TbMnO_3$ by neutron diffraction. The ordering process of the magnetic moments are summarized as follows: At $T_N^{\rm Mn} = 46$ K, the Mn moments shows a sinusoidally modulated A-type ordering with a propagation vector $(0, q_{\rm Mn}, 0)$, as reported by Quezel *et al.*[1] In addition, small G, C, and F-type with the same propagation vector coexist. $q_{\rm Mn}$ is $\sim$0.29 at $T_N^{\rm Mn}$, and smoothly decreases as the temperature is lowered showing a weak anomaly at 38 K. At $T_{\rm lock} = 28$ K, $q_{\rm Mn}$ locks at $0.276 \approx 5/18$ or $11/40$. The locking of the wave vector amplifies the Mn moment, especially enhances the G, C, and F-type components, and squares the spin arrangements. The Tb moments order below $T_N^{\rm Tb} = 7$ K, which promotes the development of the additional Mn components.

The authors thank S. Ishihara and K. Hirota for valuable discussions and critical reading of the manuscript. This work was supported by KAKENHI from the MEXT, Japan.

* Present address: Los Alamos National Laboratory, Los Alamos, New Mexico 87545, USA.

[1] S. Quezel, F. Tcheou, J. Rossat-Mignod, G. Quezel, and E. Roudaut, Physica B **86-88**, 916 (1977).
[2] J. Blasco, C. Ritter, J. García, J. M. de Teresa, J. Pérez-Cacho, and M. R. Ibarra, Phys. Rev. B **62**, 5609 (2000).
[3] A. Munõz, M. T. Casáis, J. A. Alonso, M. J. Martínez-Lope, J. L. Martínez, M. T. Fernández-Díaz, Inorg. Chem. **40**, 1020 (2001).
[4] H. W. Brinks, J. Rodríguez-Carvajal, H. Fjellvåg, A. Kjekshus, and B. C. Hauback, Phys. Rev. B **63**, 094411 (2001).
[5] A. Muñoz, J. A. Alonso, M. T. Cassais, M. J. Martínez-Lope, J. L. Martínez, and M. T. Fernández-Díaz, J. Phys.: Condens. Matter **14**, 3285 (2002).
[6] T. Kimura, S. Ishihara, H. Shintani, T. Arima, K. T. Takahashi, K. Ishizaka, and Y. Tokura, Phys. Rev. B **68**, 060403(R) (2003).
[7] T. Kimura, T. Goto, H. Shintani, K. Ishizaka, T. Arima, and Y. Tokura, Nature (London) **426**, 55 (2003).
[8] R. Kajimoto, H. Mochizuki, H. Yoshizawa, H. Shintani, T. Kimura, and Y. Tokura, in preparation.
[9] T. Chattopadhyay, P. Burlet, J. Rossat-Mignod, H. Bartholin, C. Vettier, and O. Vogt, Phys. Rev. B

49, 15096 (1994).
[10] R. Pynn, W. Press, S. M. Shapiro, S. A. Werner, Phys. Rev. B **13**, 295 (1976).